Green Chemistry

Accepted Manuscript

ROYAL SOCIETY OF CHEMISTRY

www.rsc.org/greenchem

Journal Name

ARTICLE

Ferromagnetic α-Fe_2O_3 NPs: A potential catalyst in Sonogashira Hagihara cross coupling and Hetero-Diels-Alder reactions

Received 00th January 20xx,
Accepted 00th January 20xx

DOI: 10.1039/x0xx00000x

www.rsc.org/

Meenal Kataria, Subhamay Pramanik, Navleen Kaur, Manoj Kumar, Vandana Bhalla,*

Applications of ferromagnetic *in situ* generated α-Fe_2O_3 NPs as an efficient and recyclable catalyst for carbon-carbon bond formation via Sonogashira-Hagihara coupling reactions and the synthesis of pyran derivatives by hetero-Diels-Alder reactions have been demonstrated. This catalytic system is easily recoverable due to the ferromagnetic nature of α-Fe_2O_3 NPs and can be reused with sustained selectivity and activity.

Introduction

Metal catalysed carbon-carbon (C-C) bond formation is one of most important chemical reactions in organic synthesis for efficient synthesis of natural products and heterocyclic complex molecules.[1] Consequently, for both academic and industrial purposes, development of new approaches for the formation of C-C bond is an area of great interest and hence there has been an increased emphasis on development of new catalytic systems that provide high activity in various chemical reactions.[2] Furthermore, the growing ecological concerns have motivated researchers to focus on the development of new catalytic systems which can work under eco-friendly conditions.[3] In this context, the utilization of metal nanoparticles as catalysts is one of the promising solutions to carry out reactions in mild and environmentally benign conditions and thus, a variety of homogeneous/heterogeneous catalytic systems have been developed to carry out C-C bond formation reactions.[4] Among various types of reported catalytic systems, palladium nanoparticles based systems have been found to exhibit high catalytic efficiency.[5] Though these catalytic systems contribute towards atom economy yet utilization of costly metal as major component of catalytic system remains a big hurdle towards the development of greener and sustainable chemical industry. Further, the separation and reusability of the catalytic system is another big problem. Thus, during the last few years, enormous efforts have been made to develop recoverable catalytic systems based on low priced, non-toxic and eco-friendly iron complexes for carrying out reactions involving carbon-carbon bond formation.[6] Several easy methods to assemble hybrid catalytic systems having Fe_3O_4/γ-Fe_2O_3 magnetic nanoparticles (NPs) have been reported but these catalysts impose strict limitations on the choice of only activated alkyl halides.[7] Further in most of these catalytic systems, the role of magnetic iron oxide NPs is limited to make the separation of catalytic system easy after completion of reaction and practically these nanoparticles have no contribution towards catalytic efficiency of the hybrid system.[8]

Recently, $FeCl_3$/N,N-dimethylethylenediamine and Fe_3O_4 NPs have been used as efficient catalysts to carry out Sonogashira Hagihara reaction, however, presence of high concenterations of ligand, high temperature and requirement of activated halides as reactants limit the scope of these catalytic systems.[9] Very recently, we utilized aggregates of hexaphenylbenzene derivative **1** (Figure 1) as 'not quenched' reactors and stabilizers for the preparation of ferromagnetic α-Fe_2O_3 nanoparticles at room temperature.[10] The preliminary results showed the potential of these *in situ* generated ferromagnetic α-Fe_2O_3 NPs in Pd, CuI and amine free Sonogashira cross coupling reactions. In continuation of this work, we were then interested to examine the scope of Sonogashira coupling reaction by employing different activated and inactivated halides and thus, tested a series of alkyl halides bearing various electron withdrawing and electron releasing substituents in reaction with phenylacetylene in the presence of α-Fe_2O_3 NPs. To our pleasure, all the reactions went smoothly and the corresponding products were obtained in excellent to moderate yields. Encouraged by these results, we also examined the catalytic efficiency of iron oxide nanoparticles in hetero-Diels-Alder reaction. The power of hetero-Diels-Alder reaction is universally acknowledged for construction of six membered heterocyclic compounds such as pyran derivatives.[11] However, majority of the methods for the preparation of pyran derivatives involve use of activated aldehydes. Interestingly, the α-Fe_2O_3 nanoparticles acted as efficient catalyst for converting inactivated aldehydes into stronger heterodienophiles for cycloaddition with dienes to yield various pyran derivatives. To the best of our knowledge,

[a] *Department of Chemistry, UGC Sponsored Centre for Advanced Studies-1, Guru Nanak Dev University, Amritsar 143005, and Punjab, India*
E-mail: vanmanan@yahoo.co.in † Footnotes relating to the title and/or authors should appear here.
Electronic Supplementary Information (ESI) available: [details of any supplementary information available should be included here]. See DOI: 10.1039/x0xx00000x

this is the first report where *in situ* generated ferromagnetic α-Fe_2O_3 NPs have been used as an efficient catalyst for the synthesis of pyran derivatives by Diels-Alder reaction between inactivated aldehydes and dienes. Being magnetic in nature, the separation and reuse of the ferromagnetic α-Fe_2O_3 nanoparticles is very simple, effective and economical. To the best of our knowledge, this is the first report where the utilization of *in situ* generated ferromagnetic α-Fe_2O_3 NPs have been utilized as remarkable and reusable catalyst in Sonogashira and hetero-Diels-Alder reactions.

The catalytic efficiency of these *in situ* generated α-Fe_2O_3 NPs in both Sonogashira and hetero-Diels-Alder reactions has been found to be better/ comparable to other catalytic systems reported in literature (See Supporting Information Table S1, S2 & S3).

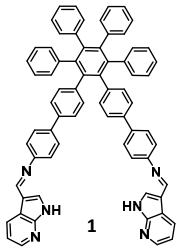

Figure 1: Hexaphenylbenzene based flourescent derivative **1** having imino groups and azaindole moieties.

Results and Discussions

The ferromagnetic α-Fe_2O_3 nanoparticles were prepared by utilizing fluorescent aggregates of hexaphenylbenzene derivative **1** as the reactors and stabilizers.[10] For preparation of these *in situ* generated nanoparticles, Fe^{3+} ions (0-25 equiv.) were added to the solution of aggregates of **1** (5 μM) in H_2O/EtOH (7:3, v/v). The reaction was stirred at room temperature for 30 min to form nanoparticles. The UV-vis spectrum showed the presence of absorption band at 395 nm and a shoulder peak at 530 nm which suggests the formation of α-Fe_2O_3 nanoparticles (See Supporting Information Figure S1). The TEM images of derivative **1** in the presence of Fe^{3+} ions showed the presence of nanorods of average length 12-18 nm (Figure 2b). We believe that the aggregates of derivative **1** reduce Fe^{3+} ions to Fe (0) state and during this process they themselves get oxidized in aqueous media. The emission spectrum of derivative **1** obtained in the presence of Fe^{3+} ions has the contribution of the oxidized species of aggregates of derivative **1**. To confirm the oxidation of aggregates of derivative **1**, we recorded the fluorescence spectrum of aggregates of derivative **1** in the presence of *tert*-butyl hydroperoxide (a strong oxidizing agent). In the fluorescence spectrum, upon addition *tert*-butyl hydroperoxide to the solution of aggregates of **1**, the fluorescence maxima at 455 nm gradually decreased and a new band appeared at 385 nm with an isoemissive point at 415 nm as was observed as in the presence of Fe^{3+} ions (See Supporting Information Figure S2 & S3). This result clearly indicates the oxidation of aggregates of derivative **1**. Further, to confirm the *in situ* formation of Fe (0) in the reaction, we carried out the UV-vis spectrum of reaction between derivative **1** and Fe^{3+} ions after keeping it under inert atmosphere. The UV-vis spectrum of the reaction mixture after 10 min showed the appearance of two bands at 265 and 350 nm corresponding to Fe (0) nanoparticles.[12] Further, on keeping the solution under aerial conditions these bands get broadened and new bands appeared at 395 and 530 nm corresponding to Fe_2O_3 nanoparticles (See Supporting Information Figure S4). To understand whether the oxidized species of derivative **1** plays any role in the formation of Fe NPs, we carried out the UV-vis studies of oxidized species of derivative **1** (prepared by adding *tert*-butyl hydroperoxide to the solution of aggregates of derivative **1**) in H_2O/EtOH (7 : 3, v/v) in the presence of Fe^{3+} ions. No absorption bands corresponding to α-Fe_2O_3 NPs were observed in the UV-vis spectrum (See Supporting Information, Figure S5). This result indicates that oxidized form of derivative **1** plays no role in the formation of α-Fe_2O_3 NPs.

To determine the structure of the oxidized species of derivative **1**, we slowly evaporated the solution of derivative **1** containing α-Fe_2O_3 NPs. After 2 days, precipitates were obtained which were filtered and washed with THF. The ^{1}H NMR spectrum of the residue so obtained after evaporation of THF solution showed the up field shift of all protons which suggests the oxidation of derivative **1**.[10] Furthermore, we carried out the reaction between derivative **1** and *tert*-butyl hydroperoxide in H_2O/EtOH (7 : 3, v/v) under lab conditions. After the completion of the reaction (TLC), the oxidized product was isolated and its structure was confirmed by spectroscopic methods. The ^{1}H NMR spectrum of the oxidized species was same as that of the organic residue (*vide supra*) left after the formation of α-Fe_2O_3 NPs (See Supporting Information, Figure S6). The FT-IR spectrum showed stretching band at 1340 cm^{-1} (ν_{N+-O-})[13] corresponding to pyridine *N*-oxide moiety (See Supporting Information, Figure S7). The ESI-MS mass spectrum showed a parent ion peak corresponding to the oxidized species of derivative **1** at m/z = 1043.5244 (See supporting information, Figure S8). These spectroscopic data corroborate the structure Ox **1** (See Supporting Information, Scheme 1) for this compound *i.e.* oxidized species of derivative **1**.

To get insight into the mechanism of formation of Fe_2O_3 nanoparticles, we studied the effect of temperature, concentration of aggregates of derivative **1** and presence of additional reducing agent such as sodium hydroxide) on the rate of formation, size and shape of iron nanoparticles. Though at high temperature and in presence of NaOH, nanorods of bigger size were obtained yet, no change in the shape of nanoparticles was observed. Upon heating the mixture of derivative **1** and Fe^{3+} ions in H_2O/EtOH (3:7, v/v) at 70°C (hydrothermal conditions), the Fe_2O_3 nanorods of size in the range of 60-80 nm were obtained (See Supporting Information, Figure S9). Further, in the presence of sodium hydroxide (pH 12), nanorods of bigger sizes were obtained rapidly (See Supporting Information, Figure S10). These studies indicate that at high temperature, and at higher pH *i.e.*, in the presence of additional reducing agents, Fe^{3+} ions undergo reduction at faster rate, hence, higher number of reduced nanoparticles are generated rapidly which are responsible for

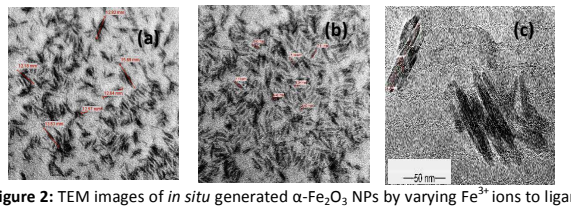

Figure 2: TEM images of *in situ* generated α-Fe_2O_3 NPs by varying Fe^{3+} ions to ligand ratio (a) 1:2, (b) 1:1, (c) 2:1

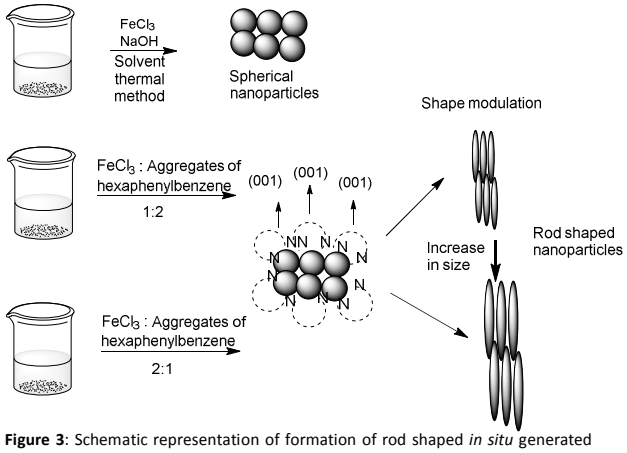

Figure 3: Schematic representation of formation of rod shaped *in situ* generated α-Fe_2O_3 nanoparticles.

furnishing nanorods of bigger size. We also studied the influence of concentration of fluorescent aggregates of hexaphenylbenzene derivative **1** in the formation of α-Fe_2O_3 nanoparticles, when Fe^{3+} ions to ligand ratio was increased from 1:1 to 2:1, an increase in the size (from 10-12 nm to 60-80 nm) of generated nanorods was observed and decrease in the size (from 10-12 nm to 4-8 nm) of nanorods was observed on switching the Fe^{3+} ions to ligand ratio from 1:1 to 1:2 (Figure 2a and 2c). Besides, UV-vis spectrum of the solution showed the red shifting of plasmon resonance, with increase in concentration of Fe^{3+} ions (See Supporting Information, Figure S11).[14] These studies suggest that plasmon resonance of α-Fe_2O_3 NPs could be fine-tuned by adjusting the amount of derivative **1**. We believe that in the presence of high concentration of aggregates of **1**, surface adsorption of nanoparticles is enhanced which inhibits the growth of nanorods.[15] Furthermore, the depletion of supply of Fe^{3+} ions in the solution also terminates the growth of nanorods. To understand the role of supramolecular aggregates of derivative **1** in enhancing the catalytic efficiency of *in situ* generated α-Fe_2O_3 NPs, we prepared α-Fe_2O_3 NPs by already reported method by using NaOH as the reducing agent.[16] The TEM and DLS studies of these generated nanoparticles showed the presence of spherical nanoparticles of size 4-6 nm (See Supporting Information, Figure S12). The Raman spectroscopic and powder XRD analysis studies confirmed the formation of α-Fe_2O_3 NPs (See Supporting Information, Figure S13 and S14). These results highlight the role of aggregates of **1** as shape directing agents. We believe that aggregates of hexaphenylbenzene derivative bind strongly along the (001) plane of α-Fe_2O_3 NPs through imino groups and azaindole moieties and thus, the growth of *in situ* generated NPs is not uniform along all the directions whereas spherical Nps were formed in the absence of aggregates of hexaphenylbenzene (Figure 3).[17]

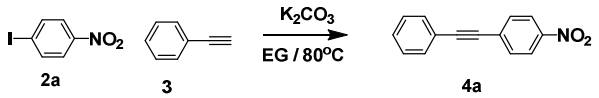

Scheme 1: Sonogashira cross coupling reaction between 4-iodo-nitrobenzene and phenyl acetylene catalysed by *in situ* generated α-Fe_2O_3 NPs.

To investigate the efficiency of *in situ* generated iron oxide nanoparticles as catalyst for C-C bond formation *via* the Sonogashira-Hagihara cross coupling reaction, 4-iodo-nitrobenzene and phenylacetylene were taken as model substrates and K_2CO_3 as a base (Scheme 1). The effect of different solvents such as ethylene glycol (EG), DMF (dimethylformamide) and DME (1,2 dimethoxyethane) was also studied by taking again 4-iodo-nitrobenzene and phenylacetylene as model substrates in the presence of 0.5 mol% of α-Fe_2O_3 NPs as catalyst and K_2CO_3 as base at 80˚C (Table 1). The yield (86%, Table 1, entry 1) was maximum when ethylene glycol was used as solvent. We believe that the hydroxyl groups of EG played an important role in stabilizing the lower oxidation state of α-Fe_2O_3 NPs during the reaction course, thus, enhancing the efficiency of the catalytic system.

To study the effect of size of α-Fe_2O_3 NPs on their catalytic efficiency, we carried out the reaction between 4-iodo-nitrobenzene and phenylacetylene using *in situ* generated α-Fe_2O_3 NPs of size (60-80 nm) (Table 1, entry 5). The reaction was complete within 27h in 86 % yield. When the same reaction was carried out by using *in situ* generated α-Fe_2O_3 NPs of size (10-14 nm / 4-8 nm) the reaction was complete in 13h (Table 1, entry 1 & 4). Thus, the increased size of Nps greatly influences the reaction rate. We also utilized the spherical α-Fe_2O_3 NPs nanoparticles generated by using NaOH

Table 1: Comparing the efficiency of *in situ* generated α-Fe_2O_3 NPs with other iron catalysts in the Sonogashira cross coupling reaction of 4-iodo-nitrobenzene with phenylacetylene.

Sr. No.	Catalyst used	Solvent	Yield (%)	Type of catalysis	Time
1	α-Fe_2O_3 NPs (Synthesized by mixing Fe^{3+}: aggregates of derivative **1**, ratio; 1:1)/size: 10-14nm	EG	86	Homogeneous	13 h
2	,,	DME	70	,,	13 h
3	,,	DMF	65	,,	13 h
4	α-Fe_2O_3 NPs (Synthesized by mixing Fe^{3+}: aggregates of derivative **1**, ratio; 1:2)/size:4:8nm	EG	88	,,	13 h
5	α-Fe_2O_3 NPs (Synthesized by mixing Fe^{3+}: aggregates of derivative **1**, ratio; 2:1)/size:60:80nm	EG	86	,,	27 h
6	Fe_2O_3 NPs (ref. 15, hydrothermal method)	EG	56	Heterogeneous	20 h
7	Fe_2O_3 NPs (ref. 15, hydrothermal method)+ Aggregates of derivative **1**	EG	58	Heterogeneous	20 h
8	$FeCl_3$	EG	22	Heterogeneous	72 h

Table 2: Effect of leaving group by using ferromagnetic *in situ* generated α-Fe_2O_3 NPs as catalyst in Sonogashira cross coupling reaction between alkyl halide and phenyl acetylene.

Entry	ArX	Alkyne	Time (h)	Temp (°C)	Product	Solvent	Isolated Yield (%)
1	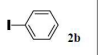 2b		18	80	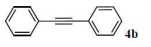 4b	EG	84
2	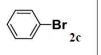 2c		24	120	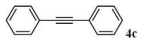 4c	EG	80
3	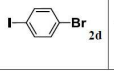 2d		18	90	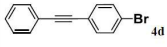 4d	EG	78

as reducing agent as heterogeneous catalysts in the reaction between 4-iodo-nitrobenzene and phenylacetylene. Under these conditions the desired product was obtained in 56% yield (Table 1, entry 6). Then, we evaluated the catalytic efficiency of α-Fe_2O_3 NPs prepared by hydrothermal method in Sonogashira cross coupling reaction of 4-iodo-nitrobenzene with phenylacetylene in the presence of derivative **1**. The reaction was complete within 20 h to yield the desired product in 58 % yield which suggests that aggregates of derivative **1** play an important role in the formation of Fe NPs (Table 1, entry 7). Furthermore, we carried out coupling reaction between 4-iodo-nitrobenzene and phenylacetylene in the presence of bulk $FeCl_3$. The reaction was sluggish and the desired product was obtained only in 22% yield in 72 h (Table 1, entry 8). These results highlight the importance of aggregates of derivative **1** in carrying out cross coupling reaction.

To check the scope of substrates, we planned to examine the reaction between aryl bromide **2c** and phenylacetylene (Table 2, entry 2). The previously reported catalytic systems exhibited low catalytic efficiency in carrying out this type of reaction.[18] To our pleasure, in the presence of *in situ* generated α-Fe_2O_3 NPs the reaction went smoothly to furnish the desired product in 80% yield (Table 2, entry 2). Furthermore, in the presence of *in situ* generated α-Fe_2O_3 NPs, 4-bromo-1-iodobenzene **2d** reacted with phenylacetylene to furnish the desired product *i.e.*, 1-bromo-4-(phenylethynyl)benzene, **4d** in 78% yield (Table 2, entry 3). These studies highlight the excellent catalytic efficiency and high selectivity of α-Fe_2O_3 NPs in the Sonogashira coupling reaction. In the next part of our work, we examined the scope of the reaction with regard to various aryl halides. Aryl halides bearing electron withdrawing subsituents underwent reaction smoothly with phenylacetylene to furnish desired products in excellent to moderate yields (Table 3, entry 1-5) and aryl halides having electron donating substituents (Table 3, entry 6-8) furnished the target molecule in moderate yields. Furthermore, 2-thiophenyl bromide also furnished the arylated alkynes in moderate yields whereas the desired product was obtained in good yield in case of 3-pyridinyl bromide (Table 3, entries 9 and 10). To further check the practical applications of *in situ* generated α-Fe_2O_3 NPs, we chose bulky electron deficient substrate 2,3-bis(4-bromophenyl)fumaronitrile **5** as the reactant. The reaction of **5**

Table 3: *In situ* generated α-Fe_2O_3 NPs catalysed Sonogashira cross coupling reaction between aromatic halides with different alkynes.

Entry	ArX	Alkyne	Time [h]	Temperature (°C)	Product	Isolated yield [%]
1	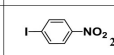 2a	 3a	13	80	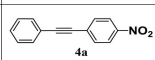 4a	86
2	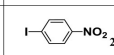 2a	 3b	13	80	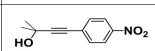 4e	85
3	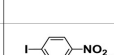 2a	 3c	20	55	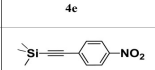 4f	80
4	 2e	 3a	18	90	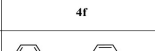 4g	72
5	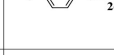 2f	 3a	18	90	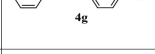 4h	70
6	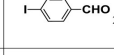 2g	 3a	18	120	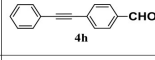 4i	68
7	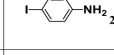 2h	 3a	24	90	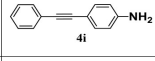 4j	64
8	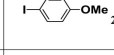 2i	 3a	24	90	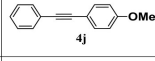 4k	62
9	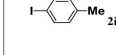 2j	 3a	20	150	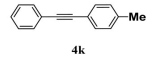 4l	60
10	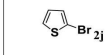 2k	 3a	24	150	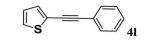 4m	76
11	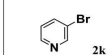 5		24	150	6	60
12	7		24	150	8	50

Reaction Conditions: Alkyl halide (1 equiv.); phenyl acetylene (1 equiv.); K_2CO_3 (2 equiv.); Ethylene Glycol; α-Fe_2O_3 NPs (0.5 mol%), Under N_2 atm.

with phenyl acetylene in ethylene glycol at 150˚C furnished the corresponding dialkynated product **6** in 60% yield (Table 3, entry 11. After that we chose bulky electron rich substrate 3-bromo-9-hexyl-9H-carbazole **7** as the reactant and allowed it to react with phenyl acetylene to furnish the corresponding product **8** in 50 % yield (Table 3, entry 12). From the above studies, it can be concluded that aggregates of derivative **1** stabilized α-Fe_2O_3 NPs exhibit high catalytic efficiency in the Sonogashira cross coupling reactions. Although electrophilicity of aryl halide is an important issue in Sonogashira-Hagihara reaction yet the fact that inactivated halide such as ary l bromide were made to react with phenylacetylene in the presence of *in situ* generated α-Fe_2O_3 NPs explains the excellent catalytic efficiency of the system in Sonogashira-Hagihara reaction.

We believe that the active Lewis acidic sites present on α-Fe_2O_3 NPs played a major role in increasing the electrophilic character of alkyl halide and C-H activation of acetylene in Sonogashira coupling reaction.[19] A plausible mechanism of *in situ* generated α-Fe_2O_3 NPs catalysed Sonogashira coupling reaction is shown in scheme 2.[20] We believe that initially aryl

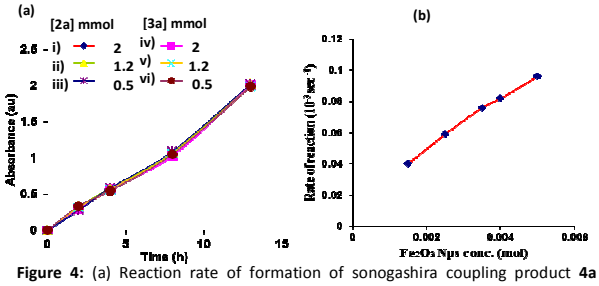

Figure 4: (a) Reaction rate of formation of sonogashira coupling product **4a** at various initial concentrations of reactants **2a:** i) 2 mmol, ii) 1.2 mmol, iii) 0.5 mmol at constant c**[3a]**; and **3a:** iv) 2 mmol, v) 1.2 mmol, vi) 0.5mmol at constant c**[2a]** ;{catalyst amount (0.5 mol %)} showed no significant change in rate constant; (b) Rate of reaction of **2a** and **3a** for the formation of **4a** at various amount of Fe_2O_3 catalyst showed linear increase with increasing amount of catalyst.

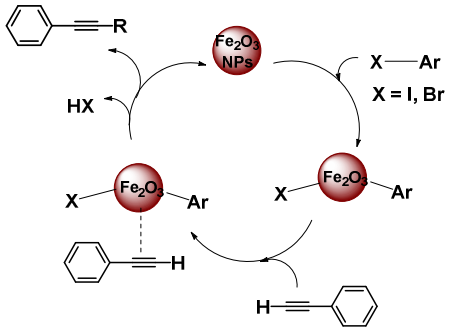

Scheme 2: Plausible catalytic cycle of α-Fe_2O_3 NPs catalysed Sonogashira cross coupling reaction.

halide interacts with the α-Fe_2O_3 NPs followed by the formation of adduct with phenyl acetylene. In the next step there might be elimination of HX to furnish the desired coupling product. Furthermore, to get insight into the mechanism about the interactions between substrates and Fe_2O_3 NPs and the formation of product, we carried out the UV-vis absorption studies.[21] We selected the reaction between 4-iodo-nitrobenzene and phenylacetylene as model reaction. The UV-vis spectra of reaction mixture **2a** and **3a** in ethylene glycol (EG) in the absence of catalyst showed the band at 292 nm. Upon the addition of Fe_2O_3 catalyst, the band at 292 nm disappeared and a new band appeared at 353 nm which suggests the interaction between the substrates and Fe_2O_3 catalyst. Then the reaction mixture was heated at 80˚C and monitored by UV-vis spectroscopy. After 30 minutes the another band corresponding to product **4a** appeared at 326 nm (See Supporting Information, Figure S15). Furthermore, we carried out the kinetic studies of Sonogashira coupling reaction between **2a** and **3a** in presence of *in situ* generated Fe_2O_3 NPs by UV-vis spectroscopy (See Supporting Information, Figure S16-21). The kinetic profiles of **2a** and **3a** at various initial concentrations (0.5 mmol to 2 mmol) and at constant catalyst amount (0.5 mol %) showed no significant change in rate constant (Figure 4a) which rule out the formation of adduct as a rate limiting step. Furthermore, kinetic measurements with different concentration of *in situ* generated α-Fe_2O_3 NPs showed a linear relationship and rate of the reaction increases with the increasing amount of catalyst (Figure 4b). These studies suggest that the rate of reaction is dependent only on the concentration of *in situ* generated α-Fe_2O_3 NPs. From above results we may conclude that the elimination of product is the rate determining step. Moreover, lower yields were obtained in case of α-Fe_2O_3 NPs prepared by using hydro thermal method and bulk $FeCl_3$ which highlights the role of aggregates of derivative **1** in enhancing the catalytic efficiency of the system (Table 1, entry 6, 7 & 8). We propose that the aggregates of derivative **1** assist in bringing the reactant molecules closer to the catalytic sites, thus, enhancing the catalytic activity of the system. Above all, the formation of small sized nanoparticles provided the large surface area for the catalytic reaction.

In the next part of our work, we examined the efficiency of *in situ* generated α-Fe_2O_3 NPs for the reaction between aryl iodide and phenyl acetylene using various amounts of catalyst. We chose the reaction between 4-iodo-nitrobenzene and phenylacetylene in ethylene glycol to examine the catalytic efficiency of catalyst. When the quantity of α-Fe_2O_3 NPs is 5000 ppm the yield is 86% in 13 h and 0% when the reaction is carried out without catalyst. Therefore, the reaction is quantitative up to 1 ppm of α-Fe_2O_3 NPs at 80˚C during 30 h (Table 4). Such an extremely low quantity of α-Fe_2O_3 NPs has never been successfully used for Sonogashira coupling reactions before the present study (See Supporting information, Table S1).

The recyclability of catalyst is a key issue from environment and synthetic point of view. We observed that α-Fe_2O_3 NPs can be easily separated by employing external magnetic field (See Supporting Information, Figure S22). From the above results, it is clear that α-Fe_2O_3 NPs can be recycled as a catalyst at least thirteen times without significant change in activity (Figure 5). After the catalytic reactions, the powder XRD studies and TEM images of recycled α-Fe_2O_3NPs revealed that size and morphology of α-Fe_2O_3 NPs did not change even after 13 cycles (See Supporting Information, Figure S23 & 24) To find out the amount of iron leached into the liquid, we carried out the atomic absorption spectroscopic (AAS) studies of the residual liquid left after the magnetic separation of catalyst and it was found that only 0.166 ppm of iron was leached into the solution (See Supporting Information, Figure S25).

Keeping in mind, the contribution of *in situ* generated α-Fe_2O_3 towards enhancement of electrophilic character of substrate, we planned to carry out hetero-Diels-Alder reaction using these NPs as a catalyst. Hetero-Diels-Alder reaction is one of most powerful synthetic organic reactions for synthesis of pyran intermediates which are the precursors of various natural products and physiologically active organic molecules. In most of the reported reactions, strong Lewis and Bronsted

Table 4: Sonogashira coupling reaction of **2a** and **3a** by using various amount of *in situ* generated α-Fe_2O_3 NPs.

Sr. No.	α-Fe_2O_3 NPs (ppm)	Time	Yield (%)	TON	TOF
1.	5000	13h	86	17.2	1.323
2.	1000	18h	85	85	4.722
3.	100	20h	83	830	41.5
4.	10	24h	82	8200	341.66
5.	1	30h	80	80000	2666.66
6.	0	0	0	0	0

acids are used to enhance the reactivity of reactants which impose a strict limitation on choice of substrates.[22] There are only few reports in literature where constructions of cyclic systems by using inactivated aldehydes have been carried out.[23] We began our investigation by choosing benzaldehyde (**9a**) and 2,3-dimethyl- 1,3-butadiene **10** as the model substrates. In the presence of the *in situ* Fe_2O_3 NPs (1 mol %), the reaction was complete in 10 h by using *p*-xylene as solvent to afford pyran derivative **14a** in 97% yield as shown in scheme **3.** For optimization of the reaction conditions we carried out the reactions in different solvents such as toluene, *p*-xylene and DCM (1, 2 dichloromethane). Lower yield were obtained in toluene and DCM but higher yields were obtained in case of *p*-xylene. Thus, we carried out all the reactions by using *p*-xylene

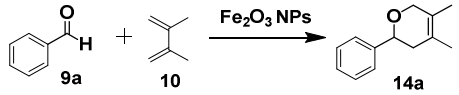

Scheme 3: Hetero Diels-Alder reaction between various aldehydes and 2, 3 dimethyl-butadiene to produce various tetrahydropyran derivatives **14a-j** catalysed by *in situ* generated α-Fe_2O_3 NPs.

Table 5: α-Fe_2O_3 NPs catalysed hetro Diels Alder reaction between diene and different aromatic and aliphatic aldehydes.

Entry	ArCHO	Time	Temp °C	Product	Yield
1.	 9a	10h	80	 14a	94%
2.	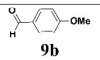 9b	10h	80	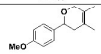 14b	85%
3.	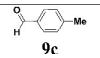 9c	10h	80	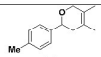 14c	93%
4.	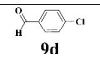 9d	10h	65	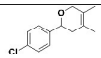 14d	90%
5.	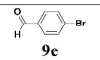 9e	10h	65	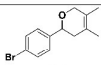 14e	88%
6.	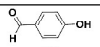 9f	10h	80	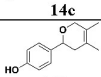 14f	82%
7.	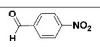 9g	16h	65	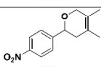 14g	86%
8.	 9h	20h	65	 14h	88%
9.	 9i	12h	80	 14i	76%
10.	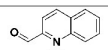 9j	12h	80	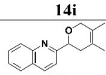 14j	78%
11.	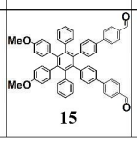 15	24 h	80	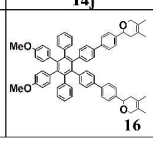 16	40%

Reaction Conditions: Aldehyde, 1 equiv.; 2,3-dimethyl-1,3-butadiene, 4equiv.; *p*-Xylene; α-Fe_2O_3 Nano catalyst, 1 mol%;

Table 6: *in situ* generated α-Fe_2O_3 NPs catalysed catalysed hetero-diels alder reaction by using various amount of catalyst:

Sr. No.	α-Fe_2O_3 NPs (ppm)	Time	Yield (%)	TON	TOF
1.	10000	10h	96	9	0.9
2.	1000	15h	95	95	6.33
3.	100	20h	94	940	47
4.	10	24h	93	9300	387.5
5.	5	30h	90	18000	600
6.	0	0	0	0	0

as solvent. Surprisingly, in the absence of solvent *i.e.*, under neat condition the desired product was also obtained in 66% yield. Both activated and inactivated aromatic aldehydes reacted smoothly to furnish the desired products **14a-j** in excellent to moderate yield (Table 5; entry 1-7). The reaction conditions are also tolerant to methoxy and hydroxyl groups. These *in situ* α-Fe_2O_3 NPs were also found to be effective catalyst for carrying out reaction between aliphatic aldehydes and diene as well as hetero-aromatic aldehydes. An acetaldehyde reacted with diene to furnish pyran derivative **14h** in 88% yield (Table 5, entry 8).

Further, to examine the regioselectivity of the catalytic system we carried out the reaction between crotonaldehyde *i.e.* α, β-unsaturated aldehyde and 2, 3-dimethyl-1,3-butadiene and the desired product **14i** was obtained in 76% yield (Table 5, entry 9). Here, the crotonaldehyde acts as a heterodienophile rather than heterodiene which proves the regioselectivity of α-Fe_2O_3 NPs in hetero-Diels–Alder reaction. Similarly under given reaction conditions 2-quinolenecarboxaldehyde also furnished the functionalized pyran derivative **14j** in 78% yield (Table 5, entry 10).

Furthermore, to explore the practical application of *in situ* generated α-Fe_2O_3 NPs, we carried out the reaction between derivative **15** and diene **10** in *p*-xylene as a solvent at 80˚C. despite the highly electron rich nature of hexaphenylbenzene derivative **15**, it underwent reaction with diene smoothly to furnish the product **16** in 40% yield (Table 5, entry 12). The efficiency of the *in situ* generated α-Fe_2O_3 NPs was tested for the reaction between hetero-Diels-Alder reaction between *p*-methylbenzaldehyde and 2, 3-dimethyl-1,3-butadiene using various amounts of α- Fe_2O_3 NPs.

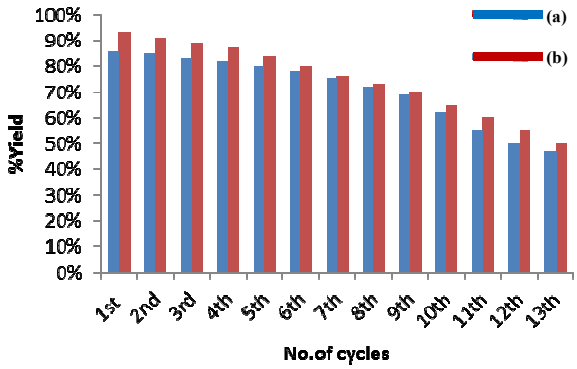

Figure 5: Recyclability of *in situ* generated α-Fe_2O_3 NPs catalyst for (a) Sonogashira coupling reaction (b) hetero-Diels-Alder reaction.

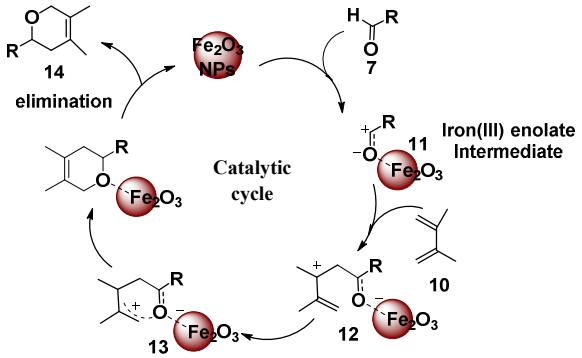

Scheme 4: Plausible catalytic cycle of Fe_2O_3 NPs catalysed Hetero-Diels-Alder reaction.

The reaction was found to be quantitative up to 5 ppm of α-Fe_2O_3 NPs during 30 h (Table 6). This high catalytic activity of *in situ* generated α-Fe_2O_3 NPs has never been seen for hetero-Diels-Alder reaction before the present study (see the Supporting Information Table S2) and its recyclability upto 13 cycles has been observed (Figure 5). A plausible mechanism is shown in scheme 4. We believe that initially aldehyde co-ordinated with iron(III) centre as axial ligands to give iron enolate intermediate **11.** The IR spectra of *p*-nitrobenzaldehyde in the presence of α-Fe_2O_3 NPs showed the shifting of band corresponding to carbonyl group to lower frequency. This might be attributed to the binding of α-Fe_2O_3 NPs with the carbonyl group of *p*-nitrobenzaldehyde (See Supporting Information, Figure S26). We believe that α-Fe_2O_3 NPs increase the electrophilicity of carbonyl bond thereby converting inactivated aldehydes into reactive heterodienophiles which hastened the cycloaddtion with diene **10**. A zwitter ionic species **12** & **13** may be formed, followed by the cyclization and further elimination of α-Fe_2O_3 to generate the desired product **14**.[24]

Conclusions

To sum up, we utilized the *in situ* generated α-Fe_2O_3 NPs for carrying out the Sonogashira coupling and hetero-Diels-Alder reactions. *In situ* generated α-Fe_2O_3 NPs were found to be effective catalyst for activated as well as inactivated substrates in case of both Sonogashira and hetero-Diels-Alder reactions. Additionally, these *in situ* generated α-Fe_2O_3 NPs catalysed the both types of reactions with high functional group tolerance and sturdiness. Being magnetic, separation of catalytic system was very easy and recyclability upto 13 cycles was observed in both Sonogashira and hetero-Diels-Alder reaction.

Experimental Section

General Experimental Procedures:

The TEM images were recorded using JEOL 2100F Transmission Electron Microscope (TEM). The FT-IR spectra were recorded with VARIAN 660 IR Spectrometer. Raman spectrum was recorded with Raneshaw in via reflex Raman microscope. ^1H and ^{13}C NMR spectra were recorded on a BRUKER-AVANCE-II FT-NMR-AL 300 and 500 MHz spectrophotometer using $CDCl_3$ as solvent and tetramethylsilane, $SiMe_4$ as internal standards. Data are reported as follows: chemical shifts in ppm, multiplicity (s = singlet, br = broad signal, d = doublet, t = triplet, m = multiplet), coupling constants *J* (Hz). Silica gel 60 (60-120 mesh) was used for column chromatography. UV-vis spectra were recorded on a SHIMADZU UV-2450 spectrophotometer, having a quartz cuvette (path length, 1 cm). The cell holder was thermostatted at 25°C. The fluorescence spectra were recorded with a SHIMADZU- 5301 PC spectrofluorimeter.

Procedure for the synthesis of *in situ* generated α-Fe_2O_3 NPs:

To a 1.0 ml solution of derivative **1** (0.15 mM) in H_2O/EtOH (7:3, v/v) was added an aqueous solution of 1.0 ml $FeCl_3$ (0.15 mM). The reaction was then stirred at room temperature for 30 minutes. The colour of reaction mixture changed from light yellow to dark yellow and the formation of α-Fe_2O_3 NPs take place. This solution containing nanoparticles (0.5-1 mol%, 100-200 µl) was used as such in the Sonogashira coupling and Hetero-Diels-Alder reactions respectively.

Synthesis of spherical α-Fe_2O_3 Nanoparticles by using reported method [15]:

0.1 M $FeCl_3$ solution was prepared by dissolving 0.162 g of $FeCl_3$ in 10 ml of water. Then, 10 ml aqueous solution of 0.3 M NaOH was added to it. The reaction mixture was stirred at room temperature for 1h to obtain yellow precipitates. After that the suspension was dried in oven at 150˚C for 2h and then cooled to room temperature. Finally, the orange-yellow precipitates were obtained which were filtered and then washed with distilled water to remove NaCl.

General procedure for Sonogashira cross coupling reactions using *in situ* generated α-Fe_2O_3 NPs as catalyst:

Aryl halide (**2a/2b/2c/2d/2e/2f/2g/2h/2i/2j/2k/5/7**; 1.0 mmol) was added to a stirred solution of *in situ* generated α-Fe_2O_3 NPs (0.5 mol%) in 1.0 ml of ethylene glycol (EG). Phenylacetylene (1.0 mmol) was then added followed by the addition of K_2CO_3 (2.0 mmol) as a base. The reaction mixture was heated under N_2 atmosphere. The reaction was monitored by using TLC. After the completion of the reaction (TLC), the reaction mixture was diluted with ethylactetate. The ethylacetate layer was washed with water (3×20 ml), dried over anhydrous Na_2SO_4 and was then removed under reduced pressure to give a crude residue. The crude residue was then purified by column chromatography using ethylacetate/hexane as eluent to give desired Sonogashira product (**4a/4b/4c/4d/4e/4f/4g/4h/4i/4j/4k/4l/4m/6/8;** Table 3). The structures of all the compounds were confirmed from their spectroscopic data (See Supporting Information, Figure S27-S40).

(4a)[6a] ^1H NMR (500 MHz, $CDCl_3$, ppm) δ = 8.22 (d, *J* = 10 Hz, 2H), 7.66 (d, *J* = 5 Hz, 2H), 7.57-7.55 (m, 2H), 7.40 (d, *J* = 5 Hz,

2H), 7.38 (dd, *J* = 5 Hz, 1H). ^{13}C NMR (125 MHz, $CDCl_3$, ppm) δ = 132.3, 131.9, 130.3, 129.3, 128.5, 123.6, 122.1, 94.7, 87.6.

(4b/4c)[6a] ^{1}H NMR (500 MHz, $CDCl_3$, ppm) δ = 7.60-7.58 (m, 4H, ArH), 7.41-7.36 (m, 6H, ArH). ^{13}C NMR (125 MHz, $CDCl_3$, ppm) δ = 131.6, 128.4, 128.3, 123.3, 89.4.

(4d)[9a] ^{1}H NMR (500 MHz, $CDCl_3$, ppm) δ = 7.57-7.55 (m, 2H, ArH), 7.51 (d, *J* = 5 Hz, 2H, ArH), 7.42 (d, *J* = 10 Hz, 2H, ArH), 7.39-7.38 (m, 3H, ArH). ^{13}C NMR (125 MHz, $CDCl_3$, ppm) δ = 133.0, 132.5, 131.6, 129.2, 128.4, 122.9, 122.3, 90.5, 88.3.

(4e) ^{1}H NMR (300 MHz, $CDCl_3$, ppm) δ = 8.16 (d, *J* = 6 Hz, 2H), 7.46 (d, *J* = 9 Hz, 2H), 4.39 (s, 1H, OH), 1.97 (s, 6H, Me). ^{13}C NMR (75 MHz, $CDCl_3$, ppm) δ = 147.0, 132.3, 131.9, 128.5, 123.6, 93.1, 84.1, 66.9, 29.7.

(4f) ^{1}H NMR (300 MHz, $CDCl_3$, ppm) δ = 8.06 (d, *J* = 9 Hz, 2H), 7.72 (d, *J* = 9 Hz, 2H), 0.24 (s, 9H, Me). ^{13}C NMR (75 MHz, $CDCl_3$, ppm) δ = 147.1, 132.4, 128.6, 123.7, 97.3, 54.3, 6.9.

(4g)[9a] ^{1}H NMR (500 MHz, $CDCl_3$, ppm) δ = 9.88 (s, 1H), 7.59 (d, *J* = 5 Hz, 2H), 7.43 (d, *J* = 5 Hz, 2H), 7.33-7.27 (m, 3H), 6.76 (d, *J* = 10 Hz, 2H). ^{13}C NMR (125 MHz, $CDCl_3$, ppm) δ = 159.2, 134.9, 132.9, 131.5, 130.7, 129.0, 128.7, 128.6, 128.2, 122.1, 114.4, 113.3, 89.7.

(4h) ^{1}H NMR (500 MHz, $CDCl_3$, ppm) δ = 9.96 (s, 1H, CHO), 7.81 (d, *J* = 10 Hz, 2H), 7.78 (d, *J* = 10 Hz, 2H), 7.60 (d, *J* = 10 Hz, 2H), 7.33-7.27 (m, 3H). ^{13}C NMR (125 MHz, $CDCl_3$, ppm) δ = 186.4, 132.4, 131.9, 130.4, 129.4, 128.6, 123.7, 122.2, 94.8.

(4i) ^{1}H NMR (300 MHz, $CDCl_3$, ppm) δ = 7.86 (d, *J* = 9 Hz, 2H), 7.70-7.62 (m, 3H), 7.48 (d, *J* = 6 Hz, 2H), 6.58 (d, *J* = 6 Hz, 2H), 4.96 (s, 2H, NH_2). ^{13}C NMR (75 MHz, $CDCl_3$, ppm) δ = 140.2, 134.4, 131.2, 130.9, 129.2, 126.8, 126.7, 125.8, 125.7, 125.6, 114.1, 112.5, 92.2, 88.8.

(4j)[9a] ^{1}H NMR (300 MHz, $CDCl_3$, ppm) δ = 7.74 (d, *J* = 9 Hz, 2H), 7.57 (d, *J* = 9 Hz, 2H), 7.48 (d, *J* = 9 Hz, 2H), 6.88 (d, *J* = 9 Hz, 3H), 3.81 (s, 3H, OMe). ^{13}C NMR (75 MHz, $CDCl_3$, ppm) δ = 159.3, 133.0, 131.9, 129.3, 127.8, 118.0, 114.2, 87.6, 56.7.

(4k)[9a] ^{1}H NMR (300 MHz, $CDCl_3$, ppm) δ = 7.52 (d, *J* = 9 Hz, 2H), 7.44-7.39 (m, 2H), 7.24-7.17 (m, 3H), 7.11-6.99 (m, 2H), 2.28 (s, 3H, Me). ^{13}C NMR (75 MHz, $CDCl_3$, ppm) δ = 138.2, 132.3, 131.9, 129.3, 128.5, 120.2, 89.8, 22.6.

(4l)[9a] ^{1}H NMR (500 MHz, $CDCl_3$, ppm) δ = 7.32 (d, *J* = 5 Hz, 1H), 7.17 (t, *J* = 7.5 Hz, 3H), 7.13 (d, *J* = 5 Hz, 2H), 6.94 (t, *J* = 5 Hz, 1H), 6.81 (d, *J* = 5 Hz, 1H). ^{13}C NMR (125 MHz, $CDCl_3$, ppm) δ = 134.4, 131.2, 130.9, 129.1, 126.7, 126.6, 125.8, 125.6, 125.4, 91.7, 88.5.

(4m)[9a] ^{1}H NMR (500 MHz, $CDCl_3$, ppm) δ = 8.67 (s, 1H), 8.45 (d, *J* = 10 Hz, 1H), 7.85 (d, *J* = 5 Hz, 1H), 7.48 (q, *J* = 5 Hz, 2H), 7.27 (dd, *J* = 5 Hz, 3H), 7.24-7.21 (m, 1H). ^{13}C NMR (125 MHz, $CDCl_3$, ppm) δ = 150.6, 147.0, 140.4, 132.3, 131.9, 130.3, 129.3, 128.5, 123.6, 122.1, 118.0, 87.6, 81.8.

(6) ^{1}H NMR (500 MHz, $CDCl_3$, ppm) δ = 7.88 (d, *J* = 10 Hz, 4H), 7.72 (d, *J* = 10 Hz, 4H), 7.71 (d, *J* = 10 Hz, 4H), 7.54-7.50 (m, 4H), 7.41 (t, *J* = 5 Hz, 2H). ^{13}C NMR (125 MHz, $CDCl_3$, ppm) δ = 132.7, 132.3, 131.8, 130.6, 130.2, 130.1, 128.7, 128.5, 126.8, 124.6, 116.1, 88.2.

(8) ^{1}H NMR (500 MHz, $CDCl_3$, ppm) δ = 8.20 (d, *J* = 10Hz, 1H, ArH), 7.89 (s, 1H, ArH), 7.60 (d, *J* = 10Hz, 4H, ArH), 7.51-7.47 (m, 4H, ArH), 7.39-7.36 (m, 1H, ArH), 7.30 (s, 1H, ArH), 4.14 (t, 2H, *J*= 7.5 Hz, -N$\underline{CH_2}$, 1.78-1.75 (m, 2H, -NCH_2-$\underline{CH_2}$), 1.39 (m, 6H, -NCH_2-CH_2-$\underline{(CH_2)_3}$-CH_3), 0.81 (t, *J*= 7.5, 3H, -$N(CH_2)_5$-CH_3. ^{13}C NMR (125 MHz, $CDCl_3$, ppm) δ = 138.9, 132.3, 129.0, 128.2, 127.7, 126.8, 125.3, 122.9, 119.5, 118.9, 115.8, 110.7, 109.7, 103.9, 92.1, 89.7, 55.4, 31.4, 29.7, 26.6, 21.4, 13.9.

General procedure for Hetero-Diels-Alder reactions using *in situ* generated α-Fe_2O_3 NPs as catalyst

1.0 mmol of aldehyde (**9a/9b/9c/9d/9e/9f/9g/9h/9i/9j/15;**) was added to stirred solution of *in situ* generated α-Fe_2O_3 NPs (1mol %) in *p*-Xylene (1.0 ml). The diene (4.0 mmol) was then added and the reaction mixture was heated for 10-24h. The progress of the reaction was monitored by TLC. After the completion of reaction (TLC), the solvent was removed under reduced pressure to obtain a crude residue to which ethylacetate was added and washed with water (3×20 ml), dried over anhydrous Na_2SO_4 and removed under reduced pressure to give a crude product. The pure product (**14a/14b/14c/14d/14e/14f/14g/14h/14i/14j/16**, Table **4**) was isolated by column chromatography using ethylacetate/ hexane as eluent. The structures of all the compounds were confirmed from their spectroscopic data (See Supporting Information, Figure S41-S52).

(14a)[11] ^{1}H NMR (500 MHz, $CDCl_3$, ppm) δ = 7.19-7.16 (m, 3H), 7.14-7.13 (m, 2H), 4.65 (dd, 1H), 4.15 (d, *J* = 10 Hz, 1H), 3.99 (d, *J* = 10 Hz, 1H), 2.31-2.26 (m, 1H), 2.04 (d, *J* = 5 Hz, 1H), 1.70 (s, 3H), 1.68 (s, 3H). ^{13}C NMR (125 MHz, $CDCl_3$, ppm) δ = 142.2, 128.8, 127.7, 127.0, 124.3, 123.6, 75.0, 71.4, 38.7, 17.9, 14.0.

(14b)[11] ^{1}H NMR (500 MHz, $CDCl_3$, ppm) δ = 7.09 (d, *J* = 10 Hz, 2H), 6.87 (d, *J* = 5 Hz, 2H),), 4.54 (dd, 1H), 3.87 (d, *J* = 10Hz, 1H), 3.81 (d, *J* = 5 Hz, 1H), 3.70 (S, 3H, OMe), 2.38-2.35 (m, 1H), 2.28-2.25 (m, 1H), 1.76 (s, 3H), 1.73 (s, 3H). ^{13}C NMR (125 MHz, $CDCl_3$, ppm) δ = 151.5, 134.6, 128.0, 124.0, 123.0, 113.9, 72.5, 70.4, 55.4, 38.1, 19.4, 12.9.

(14c)[11] ^{1}H NMR (500 MHz, $CDCl_3$, ppm) δ = 7.20 (d, J =10 Hz, 2H), 7.16 (d, *J* = 5 Hz, 2H),), 4.62 (dd, 1H), 4.34 (d, *J* = 10 Hz, 1H), 4.23 (d, *J* = 15 Hz, 1H), 2.55- 2.51 (m, 1H), 2.34 (s, 3H, Me), 2.23-2.19 (m, 1H), 1.85 (s, 6H). ^{13}C NMR (125 MHz, $CDCl_3$, ppm) δ = 139.1, 135.2, 129.0, 128.3, 125.5, 124.6, 80.0, 70.1, 31.5, 21.0, 19.2, 16.3.

(14d)[11] ^{1}H NMR (500 MHz, $CDCl_3$, ppm) δ = 7.52 (d, *J* = 5 Hz, 2H), 7.30 (d, *J* = 10 Hz, 2H),), 4.54 (dd, 1H), 4.25 (d, *J* = 15 Hz, 1H), 4.16 (d, *J* = 15 Hz, 1H), 2.38-2.26 (m, 1H), 2.14-2.10 (m, 1H), 1.74 (s, 3H), 1.64 (s, 3H), ^{13}C NMR (125 MHz, $CDCl_3$, ppm) δ = 132.8, 128.3, 127.6, 124.9, 109.8, 75.5, 70.2, 37.6, 18.3, 13.5.

(14e)[11] ^{1}H NMR 500 MHz, $CDCl_3$, ppm) δ = 7.31 (d, *J* = 5 Hz, 2H), 7.29 (d, *J* = 5 Hz, 2H), 4.67 (dd, 1H), 4.03 (d, *J* = 10 Hz, 1H), 3.91 (d, *J* = 10 Hz, 1H), 2.85-2.81 (m, 1H), 2.02 (d, 5Hz, 1H), 1.58 (s, 3H), 1.57 (s, 3H), ^{13}C NMR (125 MHz, $CDCl_3$, ppm) δ = 141.8, 131.4, 127.5, 124.6, 123.6, 121.1, 109.7, 75.5, 70.2, 38.5, 18.3, 13.8.

(14f) ^{1}H NMR (500 MHz, $CDCl_3$, ppm) δ = 9.41 (s, 1H, -OH) ,7.14 (d, *J* = 5 Hz, 2H), 7.09 (d, *J* =10 Hz, 2H), 4.54 (dd, 1H), 4.32 (d, *J* = 10Hz, 1H), 4.16 (d, *J* = 15 Hz, 1H), 2.32- 2.26 (m, 1H), 2.09 (d, *J* = 10 Hz, 1H), 1.72 (s, 3H), 1.61 (s, 3H). ^{13}C NMR (125 MHz, $CDCl_3$, ppm) δ = 156.7, 136.8, 127.6, 124.6, 123.6, 113.7, 75.6, 70.2, 38.5, 18.4, 13.9.

(14g)[11] ^{1}H NMR (500 MHz, $CDCl_3$, ppm) δ = 8.16 (d, *J* = 10 Hz, 2H), 7.57 (d, *J* = 10 Hz, 2H),), 4.57 (dd, 1H), 4.22 (d, *J* = 5 Hz, 1H), 4.03 (d, *J* = 10 Hz, 1H), 2.25-2.21 (m, 2H), 1.58 (s, 3H), 1.57 (s, 3H). ^{13}C NMR (125 MHz, $CDCl_3$, ppm) δ = 147.3, 146.4, 127.0, 124.3, 123.7, 123.6, 75.1, 70.3, 38.7, 18.4, 14.1.

(14h) ^{1}H NMR (500 MHz, $CDCl_3$, ppm) δ = 4.05 (d, *J* = 10 Hz, 1H), 4.00 (d, *J* = 10 Hz, 1H), 2.92-2.88 (m, 1H), 2.11-2.08 (m, 2H), 1.64 (s, 6H), 1.13 (s, 3H). ^{13}C NMR (125 MHz, $CDCl_3$, ppm) δ = 125.8, 122.4, 72.5, 70.4, 40.8, 21.4, 19.1, 12.8.

(14i) ^{1}H NMR (500 MHz, $CDCl_3$, ppm) δ = 5.58-5.51 (m, 2H), 4.53-4.48 (m, 2H), 3.71- 3.66 (m, 1 H), 2.41- 2.38 (m, 1H), 2.32-2.28 (m, 1H), 2.19 (s, 3H), 1.71 (s, 3H), 1.67 (s, 3H). ^{13}C NMR (125 MHz, $CDCl_3$, ppm) δ = 130.0, 128.2, 123.9, 122.8, 79.6, 70.1, 37.1, 19.8, 17.9, 12.9.

(14j) ^{1}H NMR (500 MHz, $CDCl_3$, ppm) δ = 8.34 (d, *J* = 10 Hz, 1H), 8.19 (d, *J* = 10 Hz, 1H), 8.06 (d, *J* = 10 Hz, 1H), 7.87-7.84 (m, 1H), 7.75-7.71 (m, 1H), 7.18 (d, *J* = 10 Hz, 1H), 5.03-4.94 (m, 1H), 4.10 (d, *J* = 10 Hz, 1H), 3.95 (d, *J* = 5 Hz, 1H), 2.40-2.29 (m, 1H), 2.07–2.04 (m, 1H), 1.68 (s, 3H), 1.66 (s, 3H), ^{13}C NMR (125 MHz, $CDCl_3$, ppm) δ = 152.6, 147.9, 137.4, 129.2, 128.5, 127.8, 126.5, 125.2, 124.2, 123.3, 119.1, 78.5, 69.4, 36.8, 19.2, 12.8.

(15) ^{1}H NMR (300 MHz, $CDCl_3$, ppm) δ = 10.02 (s, 2H, -CHO), 8.03 (d, *J* = 6 Hz, 4H), 7.86 (d, *J* = 6 Hz, 8H), 7.55 (d, *J* = 6Hz, 8H), 7.20 (d, *J* = 6Hz, 7.00 (d, *J* = 6Hz, 4H), 3.73 (s, 6H, -OMe)
(16) ^{1}H NMR (500 MHz, $CDCl_3$, ppm) δ = 7.69 (d, *J* = 5 Hz, 4H), 7.67 (d, *J* = 5 Hz, 4H), 7.61 (d, *J* = 10 Hz, 4H), 7.53-7.49 (m, 2H), 7.36 (d, *J* = 5 Hz, 2H), 7.21-7.18 (m, 4H), 7.16 (d, *J* = 5 Hz, 2H), 7.12 (d, *J* = 10Hz, 4H), 7.09 (d, *J* = 5Hz, 2H), 7.04 (d, *J* = 5Hz, 2H) 7.02-6.99 (m, 4H), 4.83 (dd, 2H), 4.26 (d, *J* = 5 Hz, 2H), 4.15 (d, *J* = 5 Hz, 2H), 3.17 (s, 6H), 2.29-2.26 (m, 2H), 2.15-2.13 (m, 2H), 1.66 (s, 6H), 1.64 (s, 6H). ^{13}C NMR (125 MHz, $CDCl_3$, ppm) δ = 153.5, 138.9, 132.7, 132.3, 132.2, 129.0, 128.8, 128.7, 128.2, 125.3, 124.0, 122.9, 114.4, 75.5, 65.9, 55.3, 38.1, 19.0, 13.9.

Acknowledgements

We are thankful to CSIR (ref. no. 02(0083)/12/EMR-II) for financial support. We are also thankful to UGC for UPE project. Meenal Kataria is thankful to DST for INSPIRE fellowship. Subhamay Pramanik is thankful to UGC (New Delhi) for SRF.

Notes and references

1 (a) K. Shekarrao, P. P. Kaishap, S. Gogoi and R. C. Boruaha, *Adv. Synth. Catal.,* 2015, **357**, 1187; b) A. Berkessel, E. E._rk and C. C. Laporte, *Adv. Synth. Catal*., 2006, **348**, 223; (c) B.-N. Lin, S. -H. Huang, W.-Y. Wu, C. -Y. Mou and F. -Yu. Tsai, *Molecules,* 2010, **15**, 9157; (d) R. R. Tykwinski, *Angew. Chem. Int. Ed.,* 2003, **42**, 1566; (e) J. –H. Li, J. L. Li, D. –P. Wang, S. –F. Pi, Y. –X. Xie, M. –B. Zhang and X. –C. Hu, *J. Org. Chem.*, 2007, **72**, 2053; (f) S. Cacchi and G. Fabrizi, *Chem. Rev*., 2005, **105**, 2873.

2 (a) F. Papa, I. Balint, C. Negrila, E. –A. Olaru, I. Zgura and C. Bradu, *Ind. Eng. Chem. Res*., 2014, **53**, 19094; (b) W. Xu, H. Sun, B. Yu, G. Zhang, W. Zhang and Z. Gao, *ACS Appl. Mater. Interfaces,* 2014, **6**, 2026; (c) A. Taher, D. Nandi, M. Choudhary and K. Mallick, *New J. Chem*., 2015, **39**, 5589; (d) M. Chtchigrovsky, Y. Lin, K. Ouchaou, M. Chaumontet, M. Robitzer, F. Quignard and F. Taran, *Chem. Mater.*, 2012, **24**, 1505.

3 (a) D. Srimani, S. Sawoo and A. Sarkar, *Org. Lett.,* 2007, 93639; (b) I. Hoffmann, B. Blumenröder, S. O. n. Thumann, S. Dommer and J. Schatz, *Green Chem*., 2015, **17**, 3844; (c) A. K. romi and Z.´ n Nova´k, *Chem. Commun.,* 2008, 4968.

4 (a) N.T. S. Phan, M. V. D. Sluys and C. W. Jones, *Adv. Synth. Catal.,* 2006, **348**, 609; (b) M. Lamblin, L. N. -Hardy, J. –C. Hierso, E. Fouquet and F. -X. Felpin, *Adv. Synth. Catal.,* 2010, **352**, 33; (c) S. K. Hashmi, C. Lothschütz, R. Döpp, M. Ackermann, J. D. B. Becker, M. Rudolph, C. Scholz and F. Rominger, *Adv. Synth. Catal*., 2012, **354**, 133; (d) S. T. Gadge, M. V. Khedkar, S. R. Lanke and B. M. Bhanage, *Adv. Synth. Catal*., 2012, **354**, 2049.

5 (a) M. Planellas, Y. Moglie, F. Alonso, M. Yus, R. Pleixats and A. Shafir, *Eur. J. Org. Chem.,* 2014, 3001; (b) A. L. Isfahani, I. M. -Baltork, V. Mirkhani, A. R. Khosropour, M. Moghadam and S. Tangestaninejad, *Eur. J. Org. Chem.,* 2014, 5603; (c) M. Annapurna, T. Parsharamulu, P. V. Reddy, M. Suresh, P. R. Likhar and M. L. Kantam, *Appl. Organometal. Chem.*, 2015, **29**, 234; (d) R. W. J. Scott, H. Ye, R. R. Henriquez and R. M. Crook, *Chem. Mater.,* 2003, **15**, 3873; (e) C. –W. Zhao, J. –P. Ma, Q. –K. Liu, Y. Yu, P. Wang, Y. –A. Li, K. Wang and Y. –B. Dong, *Green Chem.*, 2013, **15**, 3150.

6 (a) M. Carril, A. Correa and C. Bolm, *Angew. Chem. Int. Ed.,* 2008, **47**, 4862; (b) T. Hatakeyama, Y. Okada, Y. Yoshimoto and M. Nakamura, *Angew. Chem. Int. Ed.,* 2011, **50**, 10973; (c) K. Fujiwara, T. Kurahashi and S. Matsubara, *J. Am. Chem. Soc.,* 2012, **134**, 5512.

7 (a) C. Bolm, J. Legros, J. L. Paih and L. Zani; *Chem. Rev*., 2004, **104**, 6217; (b) K. Fujiwara, T. Kurahashi, S. Matsubara, T. Hatakeyama, Y. Okada, Y. Yoshimoto and M. Nakamura, *Angew. Chem. Int. Ed.,* 2011, **50**, 10973.

8 (a) D. Wang, C. Deraedt, L. Salmon, C. L. re, L. Etienne, J. Ruiz and D. Astruc, *Chem. Eur. J.,* 2014, **20**, 1; (b) S. R. Chaudhuri, J. Hartwig, L. Kupracz, T. Kodanek, J. Wegner and A. Kirschninga, *Adv. Synth. Catal.*, 2014, **356**, 3530; (c) F. Rajabi, S. Naserian, A. Primo and R. Luquec, *Adv. Synth. Catal.*, 2011, **353**, 2060.

9 (a) H. Firouzabadi, N. Iranpoor, M. Gholinejad and J. Hoseini, *Adv. Synth. Catal.*, 2011, **353**,125; (b) A. Wang, X. Liu, Z. Su and H. Jing; *Catal. Sci. Technol.*, 2014, **4**, 71.

10 S. Pramanik, V. Bhalla and M. Kumar, *Chem. Commun.*, 2014, **50**, 13533.

11 K. Fujiwara, T. Kurahashi, S. Matsubara, *J. Am. Chem. Soc.,* 2012, **134**, 5512.

12 K. Klačanová, P. Fodran, P. Šimon, P. Rapta, R. Boča, V. Jorík, M. Miglierini, E. Kolek, and L'. Čaplovič, *Journal of Chemistry,* 2013, **2013**, Article ID 961629.

13 Z. Shi, D. C. Koester, M. I. B.-Arapinis, and F. Glorius, *J. Am. Chem. Soc.*, 2013, **135**, 12204.

14 (a) N. Nassar and M. Husein, *phys. stat. sol.,* 2006, **6**, 203; (b) T. Wang, L. Zhang, H. Wang, W. Yang, Y. Fu, W. Zhou, W. Yu, K. Xiang, Z. Su, S. Dai and L. Chai, *ACS Appl. Mater. Interfaces*, 2013, **5**, 12449.

15 A. K. Prashar, R. P. Hodgkins, R. Kumara and R. N. Devi, *J. Mater. Chem.*, 2008, **18**, 1765.

16 W. Tang, Y. Su, Q. Li, S. Gaoa and J. K. Shanga, *J. Mater. Chem. A*, 2013, **1**, 830.

17 C. Frandsen, B. A. Legg, L. R. Comolli, H. Zhang, B. Gilbert, E. Johnsone , J. F. Banfield, *CrystEngComm.,* 2014, **16**, 1451.

18 H. Firouzabadi, N. Iranpoor, M. Gholinejad and Jafar Hoseini, *Adv. Synth. Catal.*, 2011, **353**, 125.

19 M. F. -Garcia, J. A. Rodriguez, Metal Oxide Nanoparticles, *Nanomaterials: Inorganic and Bioinorganic Perspectives*, 2007, Doi: 10.1002/0470862106.ia377.
20 (a) D. Balcells, E. Clot and O. Eisenstein, *Chem. Rev*., 2010, **110**, 749; (b) M. Karak, L. C. A. Barbosa and G. C. Hargaden, *RSC Adv*., 2014, **4**, 53442.
21 K. Grabow and U. Bentrup, *ACS Catal.*, 2014, **4**, 2153.
22 (a) H. Griengl, Geppert and K. P. Monatsh, *Chem.,* 1976, **107**, 675; (b) S. Oi, K. Kashiwagi, E. Terada, K. Ohuchi and Y. Inoue, *Tetrahedron Lett.,* 1996, **37**, 6351; (c) V. Aggarwal, G. P. Vennall, P. N. Davey and C. Newman, *Tetrahedron Lett.,* 1997, **38**, 2569; (d) T. Hanamoto, Y. Sugimoto, Z. Y. Jin and J. Inanaga, *Bull. Chem. Soc. Jpn.,* 1997, **70**, 1421.
23 K. Fujiwara, T. Kurahashi and S. Matsubara, *J. Am. Chem. Soc.,* 2012, **134**, 5512.
24 S. Oi, K. Kashlwagi, E. Terada, K. Ohuehi and Y. Inoue, *Tetrahedron Lett.,* 1996, **37**, 6351.

Graphical Abstract

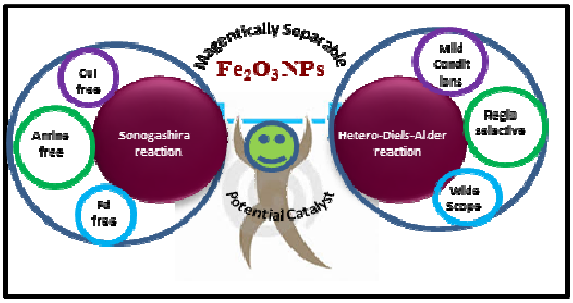

Applications of ferromagnetic *in situ* generated α-Fe_2O_3 NPs as an efficient and recyclable catalyst for carbon-carbon bond formation *via* Sonogashira-Hagihara coupling reactions and the synthesis of pyran derivatives by hetero-Diels-Alder reactions have been demonstrated. This catalytic system is easily recoverable due to the ferromagnetic nature of α-Fe_2O_3 NPs and can be reused with sustained selectivity and catalytic efficiency.